Chapter 5

On the nature and origin of the post sunset turbulence in the atmospheric boundary layer over complex terrain

5.1. Introduction

The atmospheric boundary layer becomes stably stratified after the sunset owing to the continuous cooling of the Earth's surface due to longwave radiation. Occasionally, this stability is destructed by a variety of turbulence generation mechanisms, of which dynamic instability by wind shear is considered to be the dominant and frequent mechanism. The structure of the nocturnal boundary layer (NBL) is, therefore, controlled by two competing forces of static stability and wind shear. Depending on their relative strength, the NBL falls into the quiescent regime dominated by buoyancy destruction, the continuously turbulent regime dominated by shear production, or the intermittent regime where both forcings are important (*Stull, 1988*). Increased stratification produces smaller, weaker and less efficient turbulent eddies. Turbulence in the NBL is generally weak, sporadic and occurs in bursts. These bursts recouples the surface layer to the atmosphere above and are responsible for the majority of the upward transport of heat and downward transport of momentum (*Sun et al., 2002*). These bursts primarily associated with strong wind shear can occur at any height and scale within the NBL and their dominance may vary in time and space. Thus the NBL may range from fully turbulent to intermittently turbulent or even non-turbulent at a variety of heights, temporal scales and spatial locations. It is therefore important to characterize these bursts and understand the processes responsible for their occurrence.

The structure and characteristics (winds and turbulence) of the NBL have been studied by several researchers. They include, role of the Richardson number (*Mauritsen and Svensson, 2007; Ferrero et al., 2011; Basu et al., 2014*), radiative and turbulent fluxes (*Garratt, 1981; Ha and Mahrt, 2003; Edwards, 2009*), surface heterogeneity (*Doran et al., 1995; Zhong et al., 1995; McCabe et al., 2007; Stoll. 2007; Reen et al., 2014*), large-scale subsidence (*Carlson and Stull, 1986; Mirocha and Kosovich, 2010*), baroclinicity (*Kim and Mahrt 1992*) on the structure of NBL. A number of field campaigns/experiments, such as SABLES-98 (*Cuxart et al., 2000*), CASES-99 (*Poulos et al., 2002*), SABLES 2006 (*Viana et al., 2007; Yague et al., 2007*), GABLS series (GABLS1 (*Holtslag et al., 2006*), GABLS2 (*Svensson et al., 2011*), GABLS3 (*Bosveld et al., 2014*)), WINABL (*Nappo et al., 2014*), have been conducted using a variety of instrumentation, both in situ and remote sensing to understand the horizontal and vertical structure of turbulence during the formation and evolution of NBL, and the interaction of phenomena affecting the turbulence under different heterogeneous surfaces. In particular, the occasional bursts of turbulence have been studied by several researchers and these turbulence

episodes are attributed to a variety of processes, including LLJ (*Banta et al., 2002, 2003, 2007; Ohya et al. 2008; Van de Wiel et al., 2010; Kutsher et al., 2012*), drainage flows (*Mahrt et al., 2001; Soler et al., 2002*), density currents and katabatic flows (*Papadopoulos and Helmis, 1999; Monti et al., 2002; Shapiro and Fedorovich, 2007; Shapiro et al., 2012; Shapiro and Fedorovich, 2014*), coherent structures and small-scale motions (*Cuxart et al., 2002*), meso-scale motions (*Mahrt et al., 2007*), gravity waves (*Ralph et al., 1993; Meillier et al., 2008; Sorbjan et al., 2013*), solitary waves (*Cheuang et al., 1990; Coleman et al., 2011*), inertial oscillation and nocturnal jets (*Van de Wiel et al., 2010*).

Earlier studies have shown that the turbulence on occasions persists for the whole night and on other occasions occurs as a burst. A short burst of turbulence was seen on the night of 05 October 1999 during CASES-99, which is attributed to shear instability waves *(Blumen et al. 2001)*. A detailed analysis, later, revealed that the increase in vertical shear was due to a slowing down of the flow from below (*Newsom and Banta, 2003*). *Zhou et al. (2014)* modelled several bursts of turbulence within one night and attributed them to the interaction of cold-air bubbles that are fuelled by down-valley drainage flows and shear-induced wave breaking. The cyclic process of formation and erosion is repeated during the night, leading to sporadic turbulent bursting. Recently, *Bonin et al. (2015)* have studied the spatial and temporal extent of turbulence in two categories of NBL; weakly stable NBL and very stable NBL. They noted that the turbulence is continuous in space and time within weakly stable NBL, while the turbulence variability is quite complex in very stable NBL, which is difficult to parameterize or characterize due to the intermittent nature of turbulence.

Though the above studies tried to understand the source of turbulence bursts from case studies, the statistical characteristics of these bursts are not known mainly due to the lack of sufficient suitable data. Moreover, most of the studies used the data of either instrumented meteorological tower or some remote sensing instrument. A comprehensive documentation of these episodes covering the entire ABL, from the surface to the 3-4 km, is not available in the literature. Interestingly, the time-height maps of SNR and spectral widths for case studies in Chapters 3 and 4 have clearly shown enhanced values after the sunset. We referred to them here as post-sunset turbulence (PST). Therefore, the present study aims to characterize these turbulence episodes using the data from a variety of instruments collected over 3 years and find the source(s) for these episodes. In this regard, it is important to obtain answers to the following

questions related to these turbulence episodes or PSTs: How often turbulence episodes occur during the NBL? Does PST occurs at all altitudes within the ABL or has any preferential height(s)? At what time the PST starts and how long it persists? Does it exhibit any seasonal and height dependency? Which physical mechanism is responsible for its occurrence?

This chapter is organized as follows: Section 5.2 describes the data and instrumentation employed. Section 5.3 presents the nature of PST characteristics (occurrence, start time and duration) initially through case studies later by using climatologically which also discusses the plausible source mechanism for its occurrence. The results are concluded in section 5.4.

5.2. Data and instrumentation

The present study relies on a variety of instruments, both in situ and remote sensors, whose measurements not only cover the entire NBL, but also up to 3-4 km. The data set used in the present study is same as that of in Chapter 4 and therefore not discussed here again (see section 4.2 for more details).

5.3. Results and discussion

5.3.1. A case study

A comprehensive view of the evolution of ABL in terms of surface meteorological quantities (Temperature (T), water vapor mixing ratio (r), wind speed (WS), wind variance (σ^2_{ws}) and wind direction (WD)), sodar and profiler attributes (range-corrected SNR (hereafter referred to simply as SNR), horizontal wind speed, σ, w and wind direction) on 17 May 2010 is shown in Figure 5.1, in which the vertical black solid indicates the time of sunset. Sunset on 17 May 2010 occurred at 1845 IST. The evolution of ABL is typical as described in Chapters 3 and 4 and therefore not discussed here. The striking feature, which is the subject of the present study, is the occurrence of enhanced SNR and spectral width after the sunset. Enhancement in turbulence (wind variance/spectral width) is not restricted to NBL, and is seen from the surface up to 2-2.4 km. It also persists for long time as apparent in Figure 5.1b. The intensity of the turbulence during this period is almost comparable and at times (as seen in Chapters 3 and 4) is higher than that of during the day time, when the ABL is buoyantly turbulent. This strong turbulence has the potential to recouple the surface to the atmosphere above it and therefore needs to be examined further. The two potential sources of turbulence, convective and dynamic instabilities, appear to

be present, as evidenced by strong vertical winds exceeding 1 m s^{-1} (Figure 5.1n) and horizontal winds (and wind shears) above 400 m (Figure 5.1h and m). The horizontal winds generally accelerate (Figure 5.1h) in the frictionless atmosphere above the NBL during the evening transition period and formed as a nocturnal low-level jet (NLLJ). These NLLJs are the cause for enhanced wind shears that generate turbulence. During the evening transition, the winds also change the direction at all heights within the NBL.

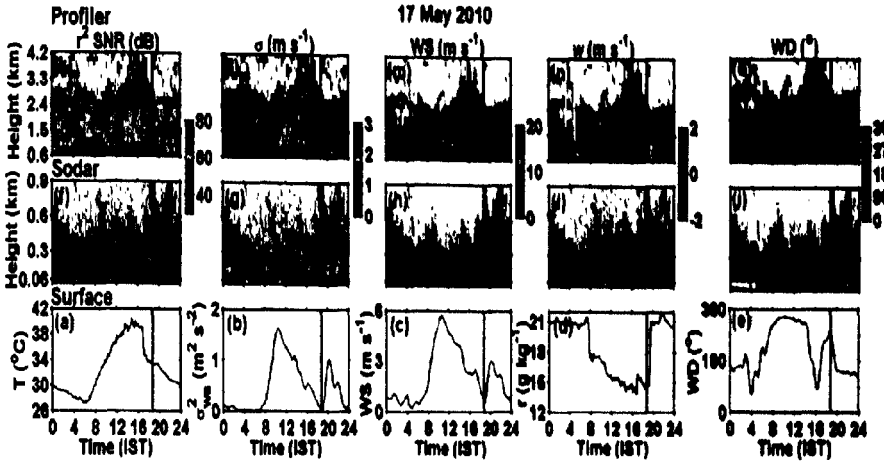

Figure 5.1: Diurnal variation of state variables at the surface and aloft on 17 May 2010. MBLM-derived surface (a) T, (b) r, (c) WS (d) σ^2_{ws} and (e) WD and sodar-derived (f) range-corrected SNR, (g) σ, (h) WS, (i) w and (j) WD. (k–o) Same as (f-j), except for profiler-derived state variables. The solid vertical line indicates the time of sunset.

5.3.2. Occurrence statistics of PST

As these turbulence episodes can occur at any height and scale, depending on the triggering process, there is a need to identify these episodes at all heights. Accordingly, measurements from surface up to 2.1 km have been used to identify the PST. The identifiers considered for PST are wind variance at the surface and spectral width aloft. First, the time series data of the above identifiers were integrated over time (5 min) and height (three heights centred on chosen level) to minimize random fluctuations. Temporal gradients of identifiers over 30 min have been estimated from 50 randomly selected days, covering all seasons. From these 50 case studies, thresholds are chosen in such a way that the algorithm should detect the start and end time of PST at all levels. The thresholds used for each identifier at surface and aloft and the procedure adopted in the present study are briefed below.

Wind variance as identifier at surface (5 m): the time at which σ^2_{ws} increases (decreases) by ≥ (≤) 0.2 $m^2 s^{-2}$ in 30 min is considered as the start (end) time of PST.

Spectral width as identifier at aloft (300 -1500 m): the time at which σ increases (decreases) by ≥ (≤) 0.2 m s^{-1} in 30 min is considered as the start (end) time of PST.

Note that all the conditions discussed above have been checked in the data collected during sunset to sunrise. The working of above procedure is tested by applying it on a case study (Figure 5.2).

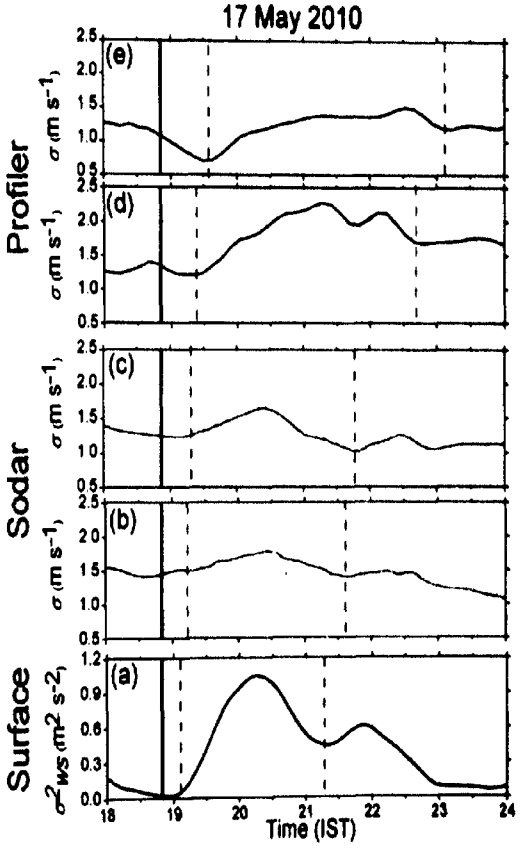

Figure 5.2: Temporal variation of MBLM-derived (a) σ^2_{ws}, (b-c) sodar-derived σ and (d-e) profiler-derived σ. The sodar- and profiler-σ are plotted at two representative levels each (300 and 450 m for sodar and 900 and 1500 m for profiler). Vertical black solid line indicates the time of sunset and vertical dashed green (cyan) lines indicate the start (end) time of PST.

On 17 May 2010, the σ^2_{ws} (Figure 5.2a) increased monotonically at the rate of ~0.5 $m^2 s^{-2}$ per 1 h from 1905 IST (green dashed line), considered as the start time of PST. It persists for longer than

2 h (in this case) before decreasing at the same rate at 2115 IST, considered as the end time of PST. The spectral width from sodar and profiler, depends primarily on irregularities in the refractive index, increases 15–30 min after the time of sunset. Interestingly, a progressive delay in the start time of PST with increasing altitude is noticed. For instance, the start time of PST observed at 1915–1920 IST in the height region of 300–450 m shifted to 1930–1935 IST in the height region of 900-1500 m (Figure 5.2b–e). The total duration of PST also increases with height; from 2 h 5 min at the surface to 3 h 25 min. at 1500 m. Clearly. the surface parameters and sodar/profiler attributes show large variations during the PST. It is also interesting to note the height dependency in both start time and duration of PST and also their systematic variation with altitude.

The occurrence statistics of PSTs, identified from the procedure stated above, are shown in Figure 5.3. In contrast to the common perception that the turbulence is occasionally breaks out during the NBL, the PSTs are ubiquitous and observed in nearly ~40–60% of total observational days at different altitudes. This indicates that there is a possibility of one PST event in two fair weather nights. The occurrence shows height dependency with relatively higher occurrence at higher altitudes (60% in the height region 900–1500 m and ~50% in the height region of 300-600 m) and lower occurrence at the surface (~38%). The occurrence of PSTs at 1500 m is ~12–15% higher than at 300 m and surface. It is not clear from the above statistics that whether PSTs occur simultaneously at all heights? Or confined to some height regions? To resolve this issue, simultaneous occurrences (surface and sodar) and independent occurrences are segregated. Among 235 nights (clear-sky nights available for the present study), PSTs are observed in both surface and sodar observations on 20% of total nights, 21% only at the surface and 26% only in sodar measurements. About 33% of nights PSTs were neither present at surface nor aloft.

The occurrence statistics show a clear seasonal dependency (Figure 5.3b) with higher occurrence during summer and lower occurrence during winter/northeast monsoon. Even during the lowest occurrence seasons, the PSTs are present on more than 20% of total days. The occurrence statistics suggest that hot and dry (cool and moist) conditions are most favorable (detrimental) for the occurrence of PSTs. The occurrence statistics clearly show the height dependency in all seasons with higher occurrence at higher altitudes than at lower altitudes. Nevertheless, the magnitude of increase in the occurrence statistics with altitude is different in different seasons. During summer, the increase is more gradual than in other seasons.

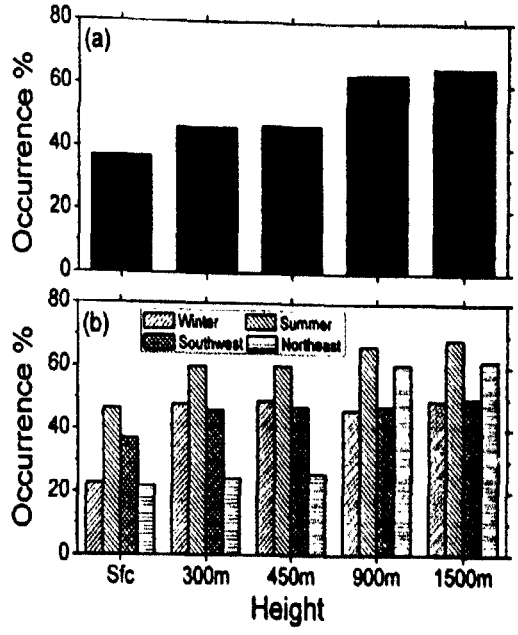

Figure 5.3: Vertical variation of PST occurrence at different levels (surface, 300, 450, 900 and 1500 m) obtained (a) from whole data and (b) in different seasons.

5.3.3. Distributions for start time and duration of PST with reference to the time of sunset

The average behaviour of the start time of PST, as identified by different identifiers (i.e., σ^2_{ws} at the surface and σ in the height region of 300-1500 m) has been studied. Figure 5.4 shows distributions of start time of PST with reference to the sunset time (PST_{sunset} = start time of PST-time of sunset) and duration of PST (end time of PST - start time of PST) at surface and chosen heights. These distributions are shown in box plots, with 25, 50, and 75 percentiles shown by the lower, middle, and upper horizontal lines of the box, respectively, and 5 and 95% of the data range by the whiskers.

It is clear from Figure 5.4 that the PSTs have a preference to occur at a particular time (depending on the height) after the sunset, as 50% of the distribution is within a period of 40 min – 1 h 15 min (25–75 percentiles). Nevertheless, the distributions are wide at all heights, indicating that the PSTs can occur as late as midnight (Figure 5.4a). Similar to the height variation observed in case study, the PST_{sunset} exhibits height dependency with a progressive delay with altitude, indicating that it follows bottom-to-top evolution. On average, the PST_{sunset}

occurs ~1 h 10 min at the surface, ~1 h 40 min in height region of 300-450 m and ~2 h in the height region of 900-1500 m, after the time of sunset.

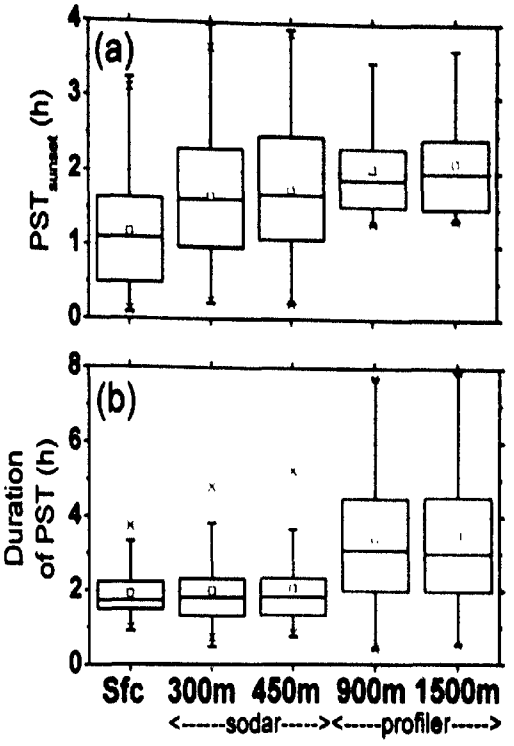

Figure 5.4: Distributions (in terms of boxplots) of (a) PST_{sunset} (= start time of PST - sunset time) (b) duration of PST (= end time of PST - start time of PST) at the surface, 300, 450, 900, and 1500 m, respectively.

Figure 5.4b clearly shows that the PST is not an instantaneous process; rather once occurs, it persists for considerable period. On average, this duration varies from 2 h at the surface to 3 h aloft. The distributions for duration at ≥ 900 m are wider than at lower heights and surface, indicating that the variability in duration is quite large at higher altitudes. At times, they persist whole night, but with varying turbulence intensity. The height variation of duration is similar to that of PST_{sunset}, with longer durations at higher altitudes. From the height variation of PST_{sunset} and duration, one can infer that the PSTs have a tilted plume structure.

A sensitivity analysis is carried out to know the impact of the above chosen thresholds on PST characteristics (occurrence, PST_{sunset} and duration of PST) as obtained by state identifier. The chosen thresholds are varied by ±20% and the mean PST characteristics obtained by state identifier is estimated at different altitudes (Figure 5.5). It is clearly shows that the statistics are

not varying much, though the thresholds are varied by ±20%. Further, the height dependence of occurrence, PST_{sunset} and duration of PST is strikingly apparent with all thresholds. It also suggests that the observed vertical variability of PST characteristics are not an artefact arising due to the chosen thresholds.

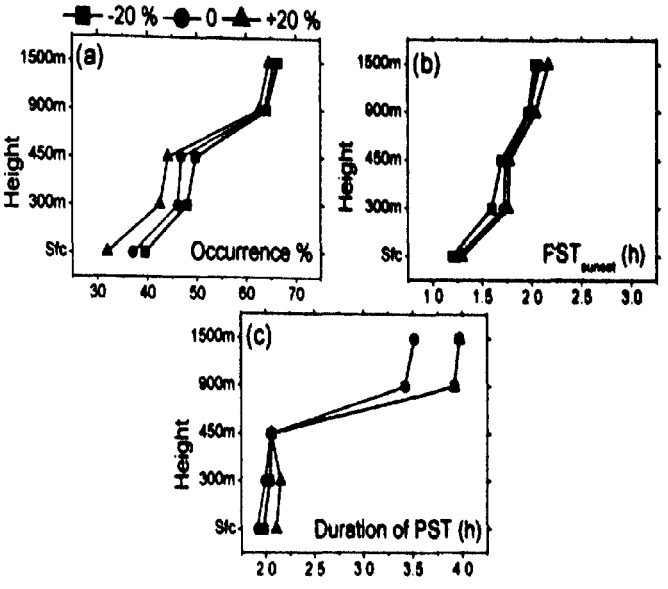

Figure 5.5: Variation of mean PST characteristics (a) occurrence (b) PST_{sunset} and (c) duration of PST as obtained for different thresholds, depicting the sensitivity of thresholds used in the present study on the PST characteristics.

5.3.4. Seasonal variation in the start time and duration of PST

The data set is segregated based on seasons and the distribution of PST_{sunset} (Figure 5.6a d) and duration of PST (Figure 5.6e–h) at different altitudes are shown in Figure 5.6. It reveals that, in the height region of 900-1500 m, the distributions for PST_{sunset} show a consistent pattern regardless of season with small variability within the season. At the surface, distribution of PST_{sunset} is consistent but it does show some seasonal variation with warm seasons showing early enhancement in turbulence (60 min after the sunset). However, the PST_{sunset} is slightly different between the seasons and also the variability is reduced (it now represents the night-to-night variability). In the height region of 300–450 m PST_{sunset} is ~1 h 30 min after the sunset and shows large variability from season to season. PST_{sunset} shows large variability in southwest monsoon season at all levels compared to other seasons. Interestingly, the PST_{sunset} also follows bottom-to-

top evolution, irrespective of season. The duration of PST also exhibits significant seasonal and vertical variability. The vertical variability in all the seasons are nearly the same with longer durations at higher levels compared to that of surface and low levels.

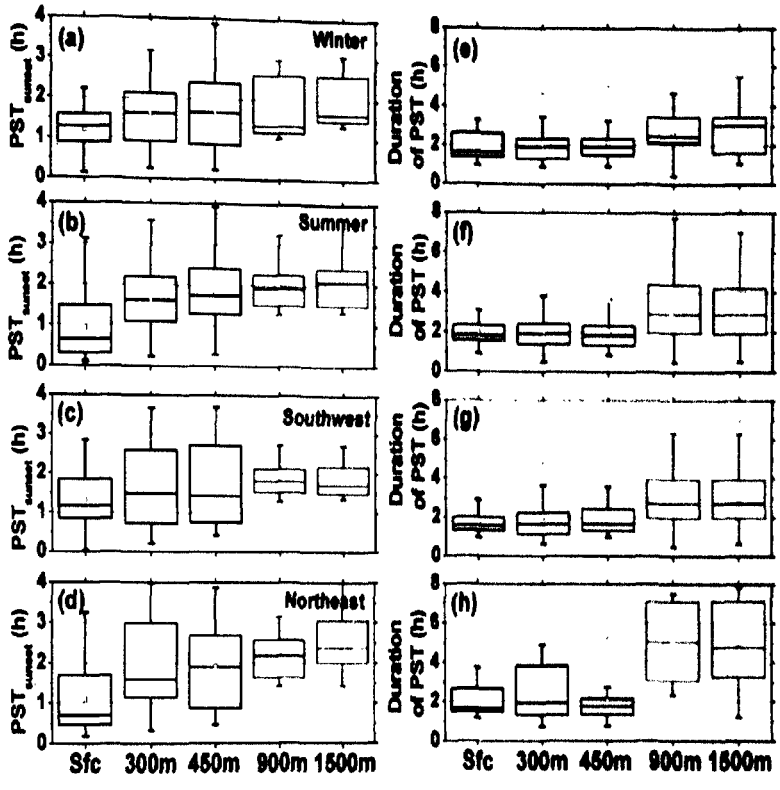

Figure 5.6: The distributions of PST_{sunset} (a-d) and duration of PST (e-h) as obtained by different identifiers for (a & e) winter (b & f) summer (c & g) southwest monsoon and (d & h) northeast monsoon.

5.3.5. Factors/mechanisms responsible for the PST occurrence

Turbulence in the lower atmospheric boundary layer depends on the diurnal heating and cooling of the ground *(Fernando et al., 2004)* and also on mechanical turbulence generated by wind shears *(Banta et al., 2007)*. During day time, the convective turbulence dominates, whereas the mechanical turbulence is predominant during the night. Nevertheless, the turbulence during the post sunset period is non-stationary and chaotic, because of weak surface forcing. An attempt has been made to understand the plausible mechanism for the occurrence of PST. To better understand the differences in the background conditions and local circulation patterns between

the post sunset turbulence nights and normal nights, composites of surface meteorological parameters for PST days and non-PST days are constructed.

From the above it is known that the start time of PST at the surface shows large night-to-night variability. To understand it, composites of different meteorological parameters are constructed with reference to the start time of PST. The variation of meteorological parameters in 6 h (2 h before to 4 h after the start time of PST) are considered. For contrasting, composites of meteorological parameters from non-PST days (or normal days) during the period 18-24 IST are considered.

5.3.5.1. Surface background conditions

Figure 5.7 depicts the mean surface background conditions (T, r, WS and σ^2_{ws}) at 5 m level between the PST (157 nights) and non-PST (267 nights) days. It is obvious that the surface conditions are drastically different during PST nights from that of non-PST nights or changing during the PST. The PST nights are clearly warmer than the non-PST nights by 4–6 °C. But both PST and non-PST nights do not show any appreciable variation at the time of PST, rather on both days the average temperature decreased monotonically. Another surface characteristic that shows significant change between PST and non-PST nights is mixing ratio (Figure 5.7b). Initially, the average (and distribution of) water vapor mixing ratio is same on nights with and without the enhanced PST at ~13 g kg^{-1}. Nevertheless, it enhanced abruptly to 16 g kg^{-1} at the time of PST on PST night, whereas it increased gradually on non-PST night. Winds generally decelerate during the afternoon transition mainly due to the reduction of downward transport of momentum *(Mahrt, 1981)*. This deceleration is seen on both days, but it continued non-PST night, but winds accelerated dramatically on PST night. Similarly, the wind variance (a form of turbulent kinetic energy) also showed marked variation between the PST and non-PST nights. As seen in case study (Figure 5.1), the increase in surface wind could be due to the formation of low-level jet. As the LLJ accelerates after the sunset, a layer of enhanced shear develops between the jet maximum and the Earth's surface generating turbulence in this layer (*Smedman, 1988; Nappo, 1991; Mahrt, 1999; Mahrt and Vickers, 2002; Banta et al., 2003; 2007*). The strength of the LLJ thus could act as a control on the magnitude of turbulence in the NBL.

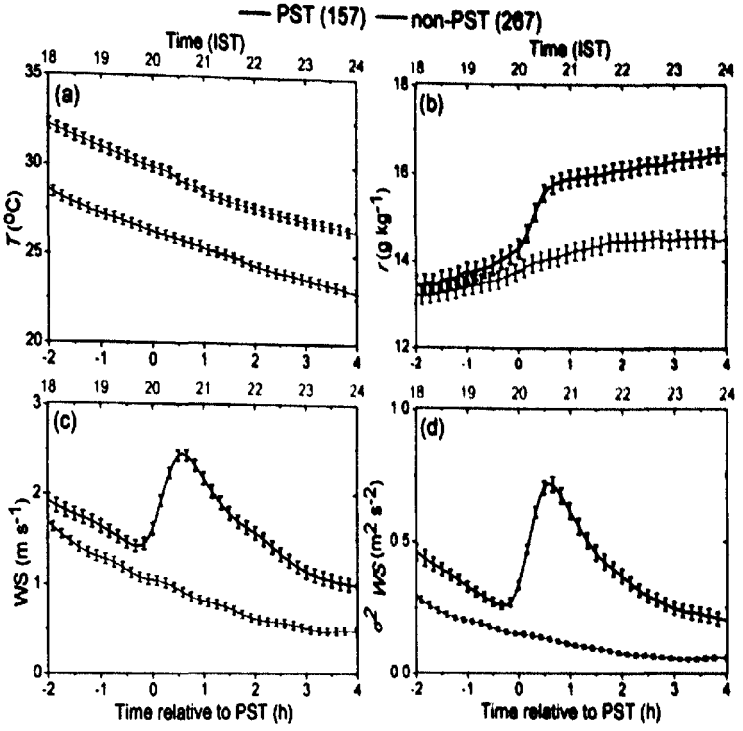

Figure 5.7: Temporal variation of mean surface state parameters (a) T, (b) r, (c) WS and (d) σ^2_{WS} during PST night (bottom axis) and non-PST night (top axis).

The increase in humidity on PST day is an interesting feature. Generally, the mixing ratio increases with the reduction in turbulence (and vice versa) because of the reduction in the upward transport of moisture by turbulence. In fact, it is one of the criteria generally followed to identify the afternoon transition (as discussed in Chapter 4). In contrast, the humidity increased on PST day, particularly at the time of PST. It means, there could be an incursion of moisture from somewhere else. Then it raises another legitimate question that which process/mechanism is responsible for the moisture incursion? Gadanki is surrounded by small hillocks and is also nearly 90 km away from the coast. It is, therefore, possible that some meso-scale circulation (like katabatic winds or sea-breeze circulation) can influence the surface meteorological parameters. But, can sea–breeze migrate as deep as 90 km? Is it the mountain induced meso-scale circulation that is bringing the moisture? To understand the source for moisture incursion, composites of wind direction during PST and non PST nights in different seasons are compared (Figure 5.8). It clearly depicts the average behaviour of local circulation on PST and non–PST nights. The flow

pattern clearly depicts the seasonal variation, but does not show any significant variation between PST and non–PST nights. Though the wind turns toward south in the late evening, but this feature is observed during both nights. It means, even if meso-scale circulations affect the surface meteorological parameters, but they do on all days. Therefore, the origin or source of moisture (enhancement) is not immediately obvious. It warrants a detailed study with intense observations and meso-scale models.

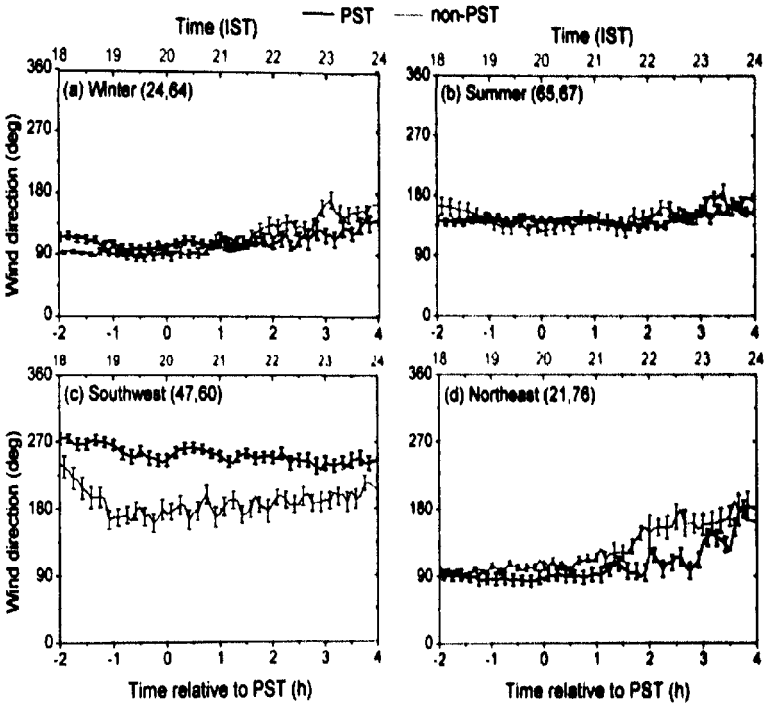

Figure 5.8: Seasonal variation in the wind direction during (a) winter, (b) summer, (c) southwest and (d) northeast at 5 m level during PST night (bottom axis) and non PST night (top axis), depicting the local circulation.

5.4. Conclusions

The anomalous behavior of turbulence occurring after the sunset at Gadanki has been characterized, in terms of their occurrence, time of occurrence, duration, height variation and seasonal variation. The major findings are as follows

1. Clearly, PSTs are not rare, rather present in nearly 40–60% of observations.

2. The occurrence shows height dependency with relatively higher occurrence at higher altitudes (60% in the height region 900–1500 m and ~50% in the height region of 300–600 m) and lower occurrence at the surface (~38%).

3. The occurrence shows seasonal dependency with higher occurrence during summer at all levels. The feature of higher occurrence of PSTs at higher altitudes is seen in all seasons. The occurrence statistics suggest that hot and dry (cool and moist) conditions are most favorable (detrimental) for the occurrence of PSTs.

4. The PST is not an instantaneous process, once occurs, persist for several hours. The duration of PST also shows height dependency with longer durations at higher altitudes.

5. Mechanisms that could explain this unexpected behavior of ABL in the absence of solar forcing is primarily associated with background conditions i.e. during the PST night the surface conditions are hotter (temperature is 4 6 °C larger than normal night), winds accelerate (no change in winds during normal night), and sudden enhancement in surface moisture.

6. The enhancement in moisture at the time of PST is surprising. The analysis suggests that there could be an incursion of moisture somewhere else. The role of meso-scale circulations is envisaged, but nearly similar wind direction on PST and non-PST nights rule out this possibility.